JOTCS B
Journal of the Turkish Chemical Society
Section: B
Chemical Engineering
TURKISH CHEMICAL SOCIETY

The Role of Stable Bicarbonate Formation on the Loss of Photocatalytic Activity of TiO_2 in Grout Media

Mert Mehmet Oymak[1], Deniz Uner*

Middle East Technical University Chemical Engineering Department, Ankara, 06531, Turkey,

Abstract: In this study, we report the photocatalytic activity of TiO_2 monitored by benzene oxidation in the grout medium. The results of the batch reaction tests indicated that the activity of TiO_2 coated on grout was substantially less than TiO_2 coated on a glass substrate. CO_2 adsorption on these samples were monitored by DRIFTS. The results reveal that the loss of activity in the grout medium was due to formation of stable carbonates-bicarbonates in highly alkaline grout media.

Keywords: Photocatalytic benzene oxidation, CO_2 Adsorption/DRIFTS, cement/grout media, dimeric form/bicarbonate, HLW/TiO_2

Submitted: August 3, 2021. **Accepted:** December 3, 2021.

Cite this: Oymak M, Uner D. The Role of Stable Bicarbonate Formation on the Loss of Photocatalytic Activity of TiO_2 in Grout Media. JOTCSB. 2022;5(1):1–8.

***Corresponding author. E-mail:** uner@metu.edu.tr.

INTRODUCTION

There is a growing market for self-cleaning and air purifying photocatalytic cementitious materials (1). Similar to cement matrix, grout matrix is also an ideal surface for photocatalytic utilization. Compared to cement matrix, grout matrices are frequently used in indoors and therefore sunlight exposure of these materials is low. However, grout applications such as patios, mosaic, stone, and tile works are aesthetic and high cost surfaces, and self-cleaning properties are desirable. Photocatalysts can be applied onto different structural supports (2), embedded in bulk (3-4). Nowadays, commercial building materials are directly coated with photocatalysts (5). The durability of the photocatalytic building materials is of both academic and commercial concern (6).

Concrete matrix, frequently encountered in buildings, is a highly alkaline environment. This high alkalinity can result in extensive amounts of CO_2 and NOx ad(ab)sorption. A recent study (7) reports that CO_2 absorption in cement matrix can compensate the CO_2 footprint of the cementitious manufacture (5). TiO_2 can also be modified with alkaline structures to increase CO_2 adsorption. Modification of TiO_2 with NH_4OH and KOH was reported to increase the total CO_2 adsorption capacity by a factor of 9 compared to the untreated sample (8). Furthermore, acidic/basic character of cementitious base materials can influence the activity of the photocatalysts. Kozlov et al. studied photocatalytic degradation of benzene and acetone with H_2SO_4 and NaOH treated samples to observe that high alkaline treatment decreased the acidic sites and photocatalytic activity of the samples (9-10). Strini et al.(11) studied photocatalytic oxidation of BTEX (Benzene, toluene, ethyl benzene and o-xylene) using P25 in Portland cement samples, comparing the activities between pure TiO_2 and TiO_2 added cementitious materials. They observed 3-10 times decrease in photocatalytic activity of P25 in cement samples when compared to pure TiO_2 activity.

Surface carbonates-bicarbonates are formed on TiO_2 surfaces under CO_2 exposure (12-21). It is known that carbon deposition changes the photocatalytic activity on TiO_2 surfaces under UV exposure or dark conditions (22). Strong Lewis acid (Ti^{4+}) and Lewis base (O^{2-}) sites favor the

1 Present address: Üsküdar University Chemical Engineering Department, İstanbul, 34662, Turkey

formation of bidentate carbonates and bicarbonate species on the surface, whereas monodentative carbonates are favored by Ti^{3+} sites (23). During photocatalytic benzene decomposition, the source of surface carbonates are the byproducts finally leading to CO and CO_2 as gaseous products (24-27).

In this article, we report activity loss due to the interactions between a commercial TiO_2 photocatalyst and its cement based environment. Our work reveals a link between carbonate-bicarbonate formation and photocatalytic activity loss on the alkaline environment of cement based samples.

EXPERIMENTAL/METHODOLOGY

A commercial TiO_2 sample (Anatase Sachtleben Hombitan LW, will be referred to as HLW from this point onwards) with a specific surface area of 11 m^2/g was used in the tests. HLW -grout sample was prepared by mixing with the grout mortar for the in-grout samples, 33 wt% water was added and the final slurry was cast in a plastic vessel (8.5 cm ID, 5 mm depth). A plain grout mortar was also prepared. The samples were cured for 28 days in a controlled atmosphere conditioned at 23 ^oC and 50% RH. On-the-grout sample was prepared by depositing 0.01 g TiO_2-deionized water solution using a syringe. On-the-glass sample was prepared by doctor blade method. The samples were air-dried for one day.

Photocatalytic benzene oxidation reaction was carried out in a homemade glass manifold (215 ml) operating in batch mode at 1 atm and room temperature. Prior to reaction measurements, the system was evacuated for 30 minutes and the reaction cell was photo-irradiated for 1 hour under vacuum. 0.2 µL of benzene was introduced to a heated manifold kept at 85 ^oC through a septum injection port and allowed to evaporate. Benzene-air mixture in gaseous form was transferred from heating system to the reaction cell through a vacuum-tight valve. The reaction products were periodically sampled through a septum by a gas-tight syringe and analyzed using a Gas Chromatograph (Varian 3900) equipped with FID and PoraplotQ capillary column. 100 W UVA (~365 nm) black light was used for photoexcitation. On the same sample, both dark and UV irradiated activities were measured. The dark experiments were done by covering the sample cell with aluminum foil while keeping the cell illuminated, to maintain identical thermal conditions.

DRIFTS (Diffuse Reflectance Infrared Fourier Transform Spectrometry) studies were performed using a Perkin Elmer (Spectrum 100 Series) Spectrometer equipped with a Pike DIFFUSIR™ DRIFTS cell connected to a home built gas manifold capable of holding vacuum up to 10^{-5} Torr connected to a Varian turbo molecular pump station. Equal amounts of samples were used in the DRIFTS cell and they were in powder form for pure TiO_2, and in the precast form for grout containing samples, which is explained in the first paragraph of experimental section. Prior to the measurements, the manifold and the cell were evacuated for 30 minutes. Subsequently, CO_2 was dosed onto sample, while monitoring the pressure by a Baratron gauge (MKS). DRIFTS spectrum was recorded after allowing system to equilibrate for 20 min. After adsorption experiments were completed, the sample was evacuated for 10 min and DRIFTS spectra were also recorded under vacuum.

RESULTS AND DISCUSSION

The photocatalytic benzene oxidation rate was measured through monitoring the concentration as a function of time (Fig. 1a). The rate estimations were based on a pseudo first order kinetics, for practical purposes without making any reference to mechanism. The time dependent disappearance of benzene from the batch reaction chamber was approximated as,

$$\ln\left(\frac{C_a}{C_{a,0}}\right) = -kt \qquad (1)$$

The reaction rate constants k can be calculated from the slope of trend lines of $\ln\left(\frac{C_a}{C_{a,0}}\right)$ vs. time graphs (Fig. 1b). The comparison of pseudo first order rate constants provides a common basis for comparing the activities of different photocatalysts and different environments (28-29).

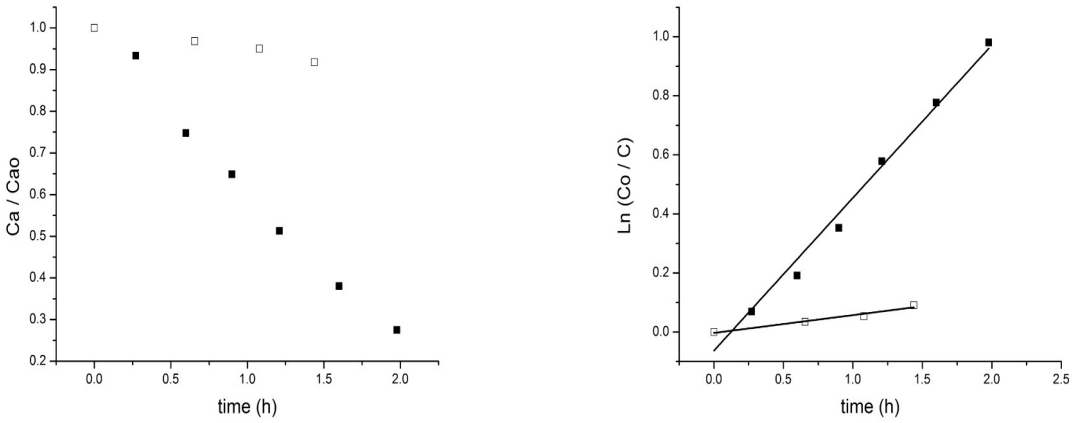

(a) **(b)**

Fig. 1: a) Benzene concentration during photocatalytic oxidation in the grout samples. The filled symbols indicate UV irradiated samples while empty symbols represent the corresponding measurements in dark. 10 wt % TiO_2 was added in the grout in both cases. b) Fig 1a is shown in the form of $\ln\left(\frac{C_{a,o}}{C_a}\right)$ vs. time.

In order to differentiate the contribution from the cement matrix, similar measurements were performed by coating the TiO_2 samples on the glass. The results were compared with the measurements of the photocatalytic activity of TiO_2 coated on the grout. The results are presented in Table 1. A comparison of the data reported in Table 1 reveals that there is substantial loss of activity on the grout.

According to the findings of an earlier publication (30) from our group, CO_2 evolution was always slower than the disappearance of C_6H_6, indicating some carbon hold-up in the structure. To test this hypothesis on the present samples, DRIFTS spectra for various HLW-grout surfaces and pure HLW and grout samples were collected (Fig. 2). IR assignments of adsorbed CO_2 on TiO_2 were made based on the literature as summarized in Table 2. The bands in DRIFTS spectra presented in Figure 2 was assigned as follows: 1800-1200 cm^{-1} region shows carbonate-bicarbonate related peaks. The absorbance in this region is low for pure grout samples. HLW integration to grout increased adsorption of CO_2 and formation of carbonates-bicarbonates substantially (Fig.2c).

Table 1: Activity comparison of HLW on glass and on grout surfaces.

	TiO_2 surface density (g/cm^2)	k_{HLW} (1/h-g cat)
On the grout	0.0005	56.6 (±16.0)
	0.0013	51.3
	0.0013	196
On the glass	0.0020	144

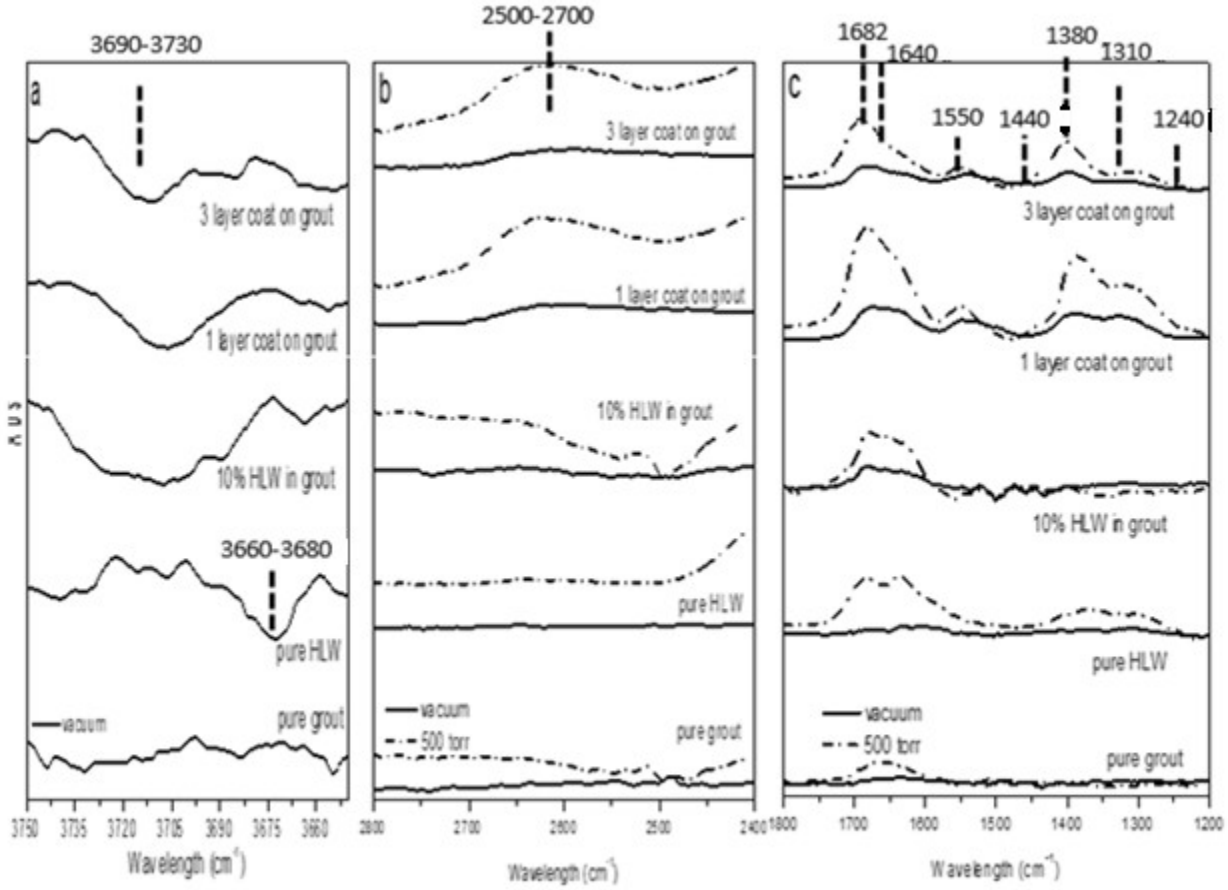

Fig. 2: DRIFTS spectra comparison of pure powder, coating and grout applications using HLW a) 3750-3650, b) 2800-2400, c) 1800-1200 cm^{-1} regions. The solid lines are collected under 500 Torr of CO_2 while dashed lines indicate the intensity after evacuation. 500 torr CO_2 data for 3750-3650 cm^{-1} region is not shown due to dominant characteristic CO_2 peaks in the region.

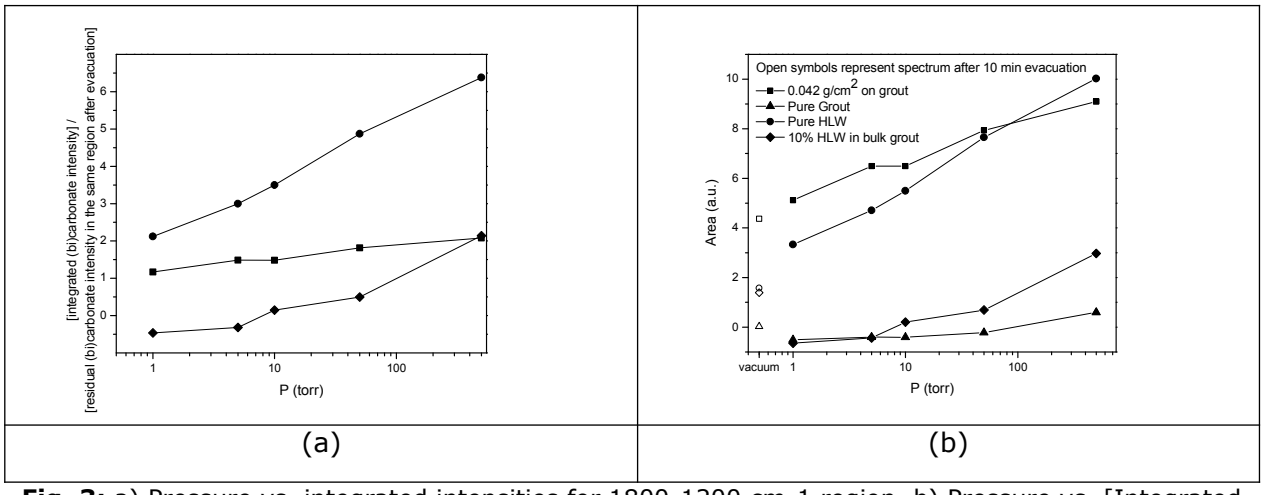

Fig. 3: a) Pressure vs. integrated intensities for 1800-1200 cm-1 region. b) Pressure vs. [Integrated (bi)carbonate intensity] / [residual (bi)carbonate intensity in the same region after evacuation]. Pure grout data in Fig 3b is not shown.

The broad peak around 2500-2700 cm^{-1} is assigned to dimeric interactions between H and OH groups of bicarbonates (Fig.2b, Table 2). This peak is observed only when HLW and grout were in intimate contact. This peak was neither observed for pure HLW nor for pure grout sample under CO_2 environment. The decrease in OH population is observed around 3700-3730 cm^{-1}

for HLW-grout and 3660-3680 cm^{-1} for pure HLW samples as negative peaks in the regions indicated. This decrease was attributed to the formation of bicarbonates over OH groups upon CO_2 adsorption. The stability of the carbonate species upon evacuation were also monitored. Surface carbonates were found to be more stable on HLW-grout than pure HLW or pure grout samples (Fig.2c). From the data in Figure 2c, it can be seen that the bands in 1200-1400 cm^{-1} range disappear upon evacuation for pure grout and 10 wt% HLW in the grout samples. These bands are however partially stable upon evacuation for pure HLW and HLW on the grout. For a semi-quantitative analysis, the area under the curve for 1800-1200 cm^{-1} region was integrated and plotted as a function of the pressure (Fig. 3a). It can be clearly seen from the isotherm data in Figure 3a that there is not an appreciable amount of (bi)carbonate hold-up on the pure grout. When TiO_2 is present, the (bi)carbonate hold-up increases (all the rest of the samples). The relative strength, i.e. stability, of the species was tested against evacuation; open symbols in Figure 3a indicate the residual intensity of the peaks after 10 min of evacuation. In Figure 3b, the isotherm data of Figure 3a (filled symbols) were plotted after they are normalized with respect to their corresponding values under vacuum (open symbols). The same data were also presented in Table 3 in terms of vacuum to 500 torr CO_2 integrated intensity ratios. The normalized values indicate that when HLW and the grout were in intimate contact, these samples hold more surface carbonate-bicarbonate species than either pure HLW or pure grout samples under vacuum conditions. However, the data presented in Fig. 3a and Fig. 2c clearly indicates that the bicarbonate formation characteristics on pure HLW and 0.042 g HLW/cm^2 coating on the grout are similar. The intensity of the bicarbonate species on pure HLW and HLW on the grout, reported in Fig. 3a, is much higher than both the corresponding intensity of pure HLW and that of HLW coated on the grout samples. The differences in the surface coverages upon evacuation were attributed to the stability of the dimeric bicarbonates.

The DRIFTS results were interpreted as there is a likelihood that a high amount of carbonate-bicarbonate species remain on TiO_2-grout matrix. The photocatalytic benzene oxidation results were interpreted as there is a significant activity loss of TiO_2 in the grout. These two observations are combined broadly to conclude that there is a surface poisoning due to stable carbonate-bicarbonate species in alkaline media.

The formation of bicarbonate species indicate the presence of basic OH groups (14). In this study, dimeric bicarbonate species were formed, which may be a sign of close proximity of OH groups on the surface of HLW-coated-grout matrix samples (Fig. 2b). These species are particularly resistant to evacuation. In addition, for the same samples, OH frequencies shift from 3660-3680 to 3730-3700 cm^{-1} region compared to pure HLW (Fig. 2a). We have to note that our measurements of reaction as well as DRIFTS were performed under conditions where water was not deliberately added to the gas streams. A recent report on an STM experiment demonstrated the importance of the film of water in CO_2 adsorption mechanism, eventually leading to formation of highly stable bicarbonates on rutile (110) (31). Furthermore, solvation effect of water decreases the energy barriers for CO_2 reduction and changes the selectivity of reaction processes on rutile (110) according to a recent first-principles calculation study (32).

A schematic representation of dimeric bicarbonate formation is given in Fig.4. Sorption takes place with initial interaction of CO_2 groups with hydroxyl groups on the surface. O-H groups make a nucleophilic attack to CO_2, forming adsorbed bicarbonate structure. This kind of bicarbonate formation is consistent with the experimental observations indicating that the OH populations decrease upon CO_2 adsorption as well.

Table 2: Peak assignments for CO_2 adsorption on TiO_2 anatase.

	Wavelength (cm^{-1})	Comments	Ref	This study
OH Stretching / Bending assignments	3735,3725,3715	ν_{OH}	10,11,12	3690-3730
	3690, 3675,3670,3665, 3640,3630(sh.)[a]	ν_{OH}	10,11, 13,12	3660-3680
	3600-3200(br.)[a]	ν_{OH} (surface and residual water)	13	3500-3000(br.)[a]
	3500-2800(br.)[a]		13	
	3350-3100(br.)[a]		10	
	1630, 1605	δ_{OH}	10,13	1640
CO_2 Assignments	3609, 3716		14	3728,3705, 3627,3600
	2375, 2360,2350, 2280[b]		12	2360,2347, 2340,2335
Carbonate / Bicarbonate Assignments	3340-3148,ν_{OH}	M–bicarbonates[c]	15	
	2620-2450,ν_{OH-O}	D-bicarbonates[c]	15	2500-2700(br.)[a]
	1702-1675,asym$\nu_{C=O}$	M–bicarbonates[c]	15	
	1672,1670	Bidentate	13,16	
	1670(sh.)[a]	Bicarbonate	14	1682
	1655-1615,asym$\nu_{C=O}$	D-bicarbonates[c]	15	
	1630	Bicarbonate	13	1640
	1632-1600	CO_3^- derivatives	10	
	1595,1578,1590-1575	Monodentate	13,16	
	1580	CO_2^- derivatives	10	1550
	1555	Bicarbonate	14	
	1410-1300	CO_3^- derivatives	10	
	1400-1370,symm$\nu_{C=O}$	D-bicarbonates[c]	15	
	1430,1420,1408	Bicarbonate	14,13	1440
	1370-1320,1359,1315	Monodentate	13,16	1380
	1346-1327,symm$\nu_{C=O}$,	M–bicarbonates[c]	15	
	1340	Bicarbonate	14	
	1320	CO_2^- derivatives	10	1310
	1300,δ_{OH-O}	D-bicarbonates[c]	15	
	(1252-1205,δ_{OH})	M–bicarbonates[c]	15	
	1243	Bidentate	13,16	
	1221,1220	Bicarbonate	14,13	1240
	1053	Bidentate	13	

[a]br.:broad peak,sh.:shoulder,[b] $^{13}CO_2$,[c]On metal oxides, M-monomeric, D-dimeric

Table 3: Carbonate bicarbonate region integrated DRIFTS intensities under vacuum, normalized with respect to their corresponding values under 500 Torr CO_2.[a] Two pure HLW experiments are averaged.

Sample	Integrated Area (Vacuum / 500 torr CO_2)
0.042 g/cm^2 coat on grout	0.48
0.014 g/cm^2 coat on grout	0.42
10% HLW in bulk grout	0.47
Pure HLW[a]	0.21
Pure grout	0.04

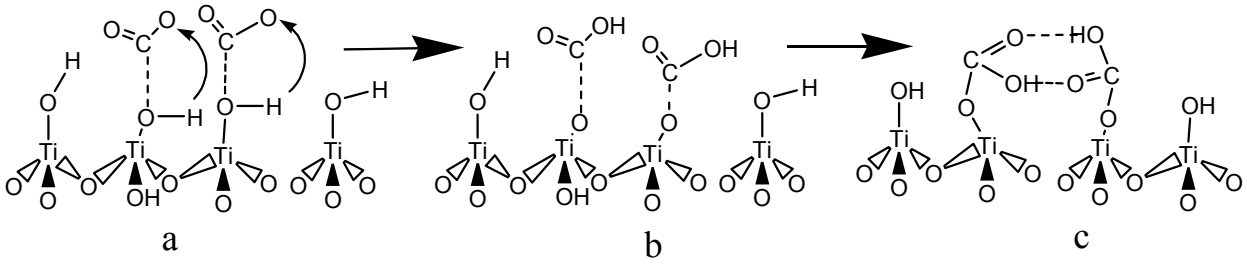

Fig. 4: Schematics of a) approach of CO_2 molecule to the surface, b) bicarbonate formation, c) dimeric bicarbonate formation.

CONCLUSIONS

The activity of the TiO_2 photocatalyst for benzene photooxidation declined by a factor of 3 when coated on a cementitious grout medium relative to the activity of a coating on a glass substrate. A detailed DRIFTS study unraveled the formation of stable carbonate-bicarbonates on TiO_2 surface in alkaline grout media. Also, dimeric bicarbonate interactions were observed on HLW-coated grout surfaces. We surmise that alkalinity in the grout can inhibit TiO_2-active sites and decrease the photocatalytic activity.

ACKNOWLEDGMENTS

Partial financial support through SANTEZ program by Kalekim A.Ş. and Turkish Ministry of Science, Industry and Technology under grant no 00336.STZ.2008-2 is acknowledged.

REFERENCES

1. M Oymak M, Uner D. Patents on photocatalyst incorporated cement based materials. Recent Patents on Catalysis (Discontinued). 2013;2(2):116–29.

2. Ramirez AM, Demeestere K, De Belie N, Mäntylä T, Levänen E. Titanium dioxide coated cementitious materials for air purifying purposes: Preparation, characterization and toluene removal potential. Building and Environment. 2010 Apr;45(4):832–8. <DOI>.

3. Aïssa AH, Puzenat E, Plassais A, Herrmann J-M, Haehnel C, Guillard C. Characterization and photocatalytic performance in air of cementitious materials containing TiO2. Case study of formaldehyde removal. Applied Catalysis B: Environmental. 2011 Aug;107(1–2):1–8. <DOI>.

4. Jimenez-Relinque E, Llorente I, Castellote M. TiO 2 cement-based materials: Understanding optical properties and electronic band structure of complex matrices. Catalysis Today. 2017 Jun;287:203–9. <DOI>.

5. Demeestere K, Dewulf J, De Witte B, Beeldens A, Van Langenhove H. Heterogeneous photocatalytic removal of toluene from air on building materials enriched with TiO2. Building and Environment. 2008 Apr;43(4):406–14. <DOI>.

6. Boonen E, Beeldens A, Dirkx I, Bams V. Durability of Cementitious Photocatalytic Building Materials. Catalysis Today. 2017 Jun;287:196–202. <DOI>.

7. Xi F, Davis SJ, Ciais P, Crawford-Brown D, Guan D, Pade C, et al. Substantial global carbon uptake by cement carbonation. Nature Geosci. 2016 Dec;9(12):880–3. <DOI>.

8. Kapica-Kozar J, Kusiak-Nejman E, Wanag A, Kowalczyk Ł, Wrobel RJ, Mozia S, et al. Alkali-treated titanium dioxide as adsorbent for CO2 capture from air. Microporous and Mesoporous Materials. 2015 Jan;202:241–9. <DOI>.

9. Kozlov D, Bavykin D, Savinov E. Effect of the Acidity of TiO2 Surface on Its Photocatalytic Activity in Acetone Gas-Phase Oxidation. Catalysis Letters. 2003;86(4):169–72. <DOI>.

10. Kozlov DV, Panchenko AA, Bavykin DV, Savinov EN, Smirniotis PG. Influence of humidity and acidity of the titanium dioxide surface on the kinetics of photocatalytic oxidation of volatile organic compounds. Russian Chemical Bulletin. 2003;52(5):1100–5. <DOI>.

11. Strini A, Cassese S, Schiavi L. Measurement of benzene, toluene, ethylbenzene and o-xylene gas phase photodegradation by titanium dioxide dispersed in cementitious materials using a mixed flow reactor. Applied Catalysis B: Environmental. 2005 Oct;61(1–2):90–7. <DOI>.

12. Yates D. Infrared studies of the surface hydroxyl groups on titanium dioxide, and of the chemisorption of carbon monoxide and carbon dioxide. The Journal of Physical Chemistry. 1961;65(5):746–53.

13. Primet M, Pichat P, Mathieu MV. Infrared study of the surface of titanium dioxides. I.

Hydroxyl groups. The Journal of Physical Chemistry. 1971;75(9):1216–20.

14. Busca G, Saussey H, Saur O, Lavalley JC, Lorenzelli V. FT-IR characterization of the surface acidity of different titanium dioxide anatase preparations. Applied Catalysis. 1985 Jan;14:245–60. <DOI>.

15. Martra G. Lewis acid and base sites at the surface of microcrystalline TiO2 anatase: relationships between surface morphology and chemical behaviour. Applied Catalysis A: General. 2000 Aug;200(1–2):275–85. <DOI>.

16. Mathieu MV, Primet M, Pichat P. Infrared study of the surface of titanium dioxides. II. Acidic and basic properties. The Journal of Physical Chemistry. 1971;75(9):1221–6.

17. Busca G, Lorenzelli V. Infrared spectroscopic identification of species arising from reactive adsorption of carbon oxides on metal oxide surfaces. Materials Chemistry. 1982 Jan;7(1):89–126. <DOI>.

18. Morterra C, Chiorino A, Boccuzzi F, Fisicaro E. A Spectroscopic Study of Anatase Properties. Zeitschrift für Physikalische Chemie. 1981 Feb 1;124(2):211–22. <DOI>.

19. Tanaka K, White J. Characterization of species adsorbed on oxidized and reduced anatase. The Journal of Physical Chemistry. 1982;86(24):4708–14.

20. Ramis G, Busca G, Lorenzelli V. Low-temperature CO2 adsorption on metal oxides: spectroscopic characterization of some weakly adsorbed species. Materials Chemistry and Physics. 1991 Sep;29(1–4):425–35. <DOI>.

21. Bhattacharyya K, Danon A, K.Vijayan B, Gray KA, Stair PC, Weitz E. Role of the Surface Lewis Acid and Base Sites in the Adsorption of CO 2 on Titania Nanotubes and Platinized Titania Nanotubes: An in Situ FT-IR Study. J Phys Chem C. 2013 Jun 20;117(24):12661–78. <DOI>.

22. Uner D, Oymak MM. On the mechanism of photocatalytic CO2 reduction with water in the gas phase. Catalysis Today. 2012 Feb;181(1):82–8. <DOI>.

23. Wu W, Bhattacharyya K, Gray K, Weitz E. Photoinduced Reactions of Surface-Bound Species on Titania Nanotubes and Platinized Titania Nanotubes: An in Situ FTIR Study. J Phys Chem C. 2013 Oct 10;117(40):20643–55. <DOI>.

24. Jacoby WA, Blake DM, Penned JA, Boulter JE, Vargo LM, George MC, et al. Heterogeneous Photocatalysis for Control of Volatile Organic Compounds in Indoor Air. Journal of the Air & Waste Management Association. 1996 Sep;46(9):891–8. <DOI>.

25. d'Hennezel O, Pichat P, Ollis DF. Benzene and toluene gas-phase photocatalytic degradation over H2O and HCL pretreated TiO2: by-products and mechanisms. Journal of Photochemistry and Photobiology A: Chemistry. 1998 Nov;118(3):197–204. <DOI>.

26. Wu W-C, Liao L-F, Lien C-F, Lin J-L. FTIR study of adsorption, thermal reactions and photochemistry of benzene on powdered TiO2. Phys Chem Chem Phys. 2001;3(19):4456–61. <DOI>.

27. Zhong J, Wang J, Tao L, Gong M, Zhimin L, Chen Y. Photocatalytic degradation of gaseous benzene over TiO2/Sr2CeO4: Kinetic model and degradation mechanisms. Journal of Hazardous Materials. 2007 Jan;139(2):323–31. <DOI>.

28. Lachheb H, Puzenat E, Houas A, Ksibi M, Elaloui E, Guillard C, et al. Photocatalytic degradation of various types of dyes (Alizarin S, Crocein Orange G, Methyl Red, Congo Red, Methylene Blue) in water by UV-irradiated titania. Applied Catalysis B: Environmental. 2002 Nov;39(1):75–90. <DOI>.

29. Stylidi M, Kondarides D, Verykios X. Pathways of solar light-induced photocatalytic degradation of azo dyes in aqueous TiO2 suspensions. Applied Catalysis B: Environmental. 2003 Feb 28;40(4):271–86. <DOI>.

30. Uner DO, Ozbek S. The deactivation behavior of the TiO2 used as a photo-catalyst for benzene oxidation. In: Studies in Surface Science and Catalysis [Internet]. Elsevier; 1999 [cited 2021 Dec 6]. p. 411–4. <URL>.

31. Song A, Skibinski ES, DeBenedetti WJI, Ortoll-Bloch AG, Hines MA. Nanoscale Solvation Leads to Spontaneous Formation of a Bicarbonate Monolayer on Rutile (110) under Ambient Conditions: Implications for CO 2 Photoreduction. J Phys Chem C. 2016 May 5;120(17):9326–33. <DOI>.

32. Yin W-J, Krack M, Wen B, Ma S-Y, Liu L-M. CO 2 Capture and Conversion on Rutile TiO 2 (110) in the Water Environment: Insight by First-Principles Calculations. J Phys Chem Lett. 2015 Jul 2;6(13):2538–45. <DOI>.